

Accepted Manuscript

Research paper

Effect of Dimethylaminophenyl and Thienyl donor groups on Zn-Porphyrin for Dye Sensitized Solar Cell (DSSC) Applications

S. Kotteswaran, V. Mohankumar, M. Senthil Pandian, P. Ramasamy

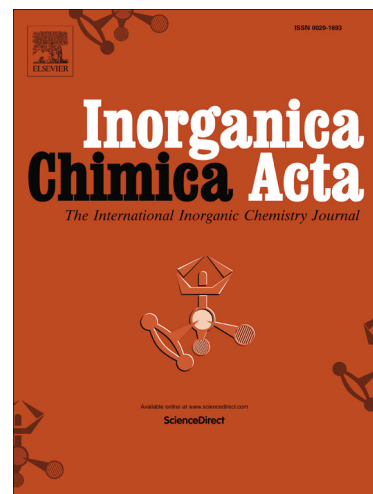
PII: S0020-1693(17)30920-9
DOI: <http://dx.doi.org/10.1016/j.ica.2017.08.020>
Reference: ICA 17814

To appear in: *Inorganica Chimica Acta*

Received Date: 10 June 2017
Revised Date: 9 August 2017
Accepted Date: 10 August 2017

Please cite this article as: S. Kotteswaran, V. Mohankumar, M.S. Pandian, P. Ramasamy, Effect of Dimethylaminophenyl and Thienyl donor groups on Zn-Porphyrin for Dye Sensitized Solar Cell (DSSC) Applications, *Inorganica Chimica Acta* (2017), doi: <http://dx.doi.org/10.1016/j.ica.2017.08.020>

This is a PDF file of an unedited manuscript that has been accepted for publication. As a service to our customers we are providing this early version of the manuscript. The manuscript will undergo copyediting, typesetting, and review of the resulting proof before it is published in its final form. Please note that during the production process errors may be discovered which could affect the content, and all legal disclaimers that apply to the journal pertain.



Effect of Dimethylaminophenyl and Thienyl donor groups on Zn-Porphyrin for Dye Sensitized Solar Cell (DSSC) Applications

S. Kotteswaran, V. Mohankumar, M. Senthil Pandian, P. Ramasamy

SSN Research Centre SSN College of Engineering, Kalavakkam, Chennai-603110, Tamilnadu.

Email of the corresponding author – kotties555@gmail.com

Abstract

We have designed and synthesized two Zn-Porphyrin derivatives Zn[5,15-dimethylaminophenyl-10,20-(4-carboxyphenyl)Porphyrin] (**SKPor-1**) and Zn[5,15-thiophene-10,20-(4-carboxyphenyl)Porphyrin] (**SKPor-2**) which possess donor modified structures as sensitizer for Dye Sensitized Solar Cells (DSSCs). These molecules contain the porphyrin unit as π -bridge, dimethylaminophenyl and thienyl groups as electron donor group and carboxylic acid group as anchoring group (electron acceptor unit). The **SKPor-1** dye has large red-shift of the absorption maxima due to introduction of the dimethylaminophenyl moiety at the meso position of the porphyrin ring. But the absorption maxima of **SKPor-2** is a little red-shifted due to the thienyl group attached with the porphyrin unit. The highly conjugated dimethylaminophenyl group is efficiently donating the electrons and electronic interaction between the porphyrin and dimethylaminophenyl unit is better compared to thienyl unit. The DSSC was made using commercial P25 TiO₂ material as photoanode, Zn-Porphyrin derivatives as sensitizer, I⁻/I³⁻ as electrolyte and Platinum (Pt) as counter electrode. The highest power conversion efficiency of the two Zn-Porphyrin derivatives (**SKPor-1**) based on DSSC reached **3.2 %** with open circuit voltage (V_{oc}) of 0.68 V, short circuit photocurrent density (J_{sc}) of 9.62 mA/cm² and fill factor (ff) of 0.50, **SKPor-2** based DSSC

reached **2.5%** open circuit voltage (V_{oc}) of 0.68 V, short circuit photocurrent density (J_{sc}) of 7.2 mA/cm² and fill factor (ff) of 0.51 under AM 1.5 G irradiation.

Keywords: Zn-Porphyrin derivatives, DSSC, UV-Vis NIR spectrum, cyclic voltammetry, power conversion efficiency.

Corresponding author (S. Kotteswaran)

1. Introduction:

To maintain global economic growth and to reduce global warming and environmental pollution, the exploration of renewable energy resources is of great significance. Sunlight is the most generous resource that can bring clean and efficient energy to meet the increasing demand worldwide. Since past few years there has been more attention in photo-active molecules to convert solar energy into electrical power. Dye-sensitized solar cells (DSSCs) have been paid much more attention due to the relatively high solar energy conversion and potentially low cost [1-5]. Dye sensitized solar cells (DSSCs), based on electrochemical devices, are very good alternatives to conventional silicon based photovoltaic technologies for solar energy conversion owing to their high power conversion efficiency (PCE) and low cost of fabrication [6-7]. In dye sensitized solar cells, light is absorbed by the dye and charge separation takes place owing to photo induced electron injection from the dye into the conduction band of semiconductors, the separated charges then move towards respective electrode thereby yielding a photocurrent in an external circuit. To develop the most efficient dyes in DSSC the essential design requirements are: 1) The sensitizing dyes must strongly be adsorbed into photocatalyst (semiconductors) surface to ensure efficient electron injection into conduction band of semiconductors, 2) The lowest unoccupied molecular orbital (LUMO) of the dye must be sufficiently higher than the conduction band of semiconductors

for efficient charge injection, and the highest occupied molecular orbital (HOMO) of the dye must be lower than the redox potential for the efficient regeneration of the oxidized dye, 3) The dye must absorb in the UV, visible and IR regions of the solar spectrum. The research on dye sensitized solar cells (DSSCs) has intensified in recent years. Nowadays, DSSCs based on the ruthenium sensitizers have achieved power conversion efficiencies (η) of 12.4%. However, ruthenium dyes are expensive due to the cost of ruthenium and the typically lengthy purification steps involved in their preparation. Alternative low cost and readily accessible ruthenium dye replacements are under active investigation [8-16].

Porphyryns are one of the alternative dyes used as sensitizers with many advantages as follows. 1) Nature has chosen porphyrin-related pigments in the light-harvesting antennae of photosynthetic organisms that power biological systems. The chromophores in the photosynthetic reaction centre capture sunlight efficiently and convert solar energy into usable chemical energy. The porphyryns derived from chlorophylls which are the key components of natural photosynthetic systems in green plants and absorb strongly in the range of 400 - 700 nm with high molar absorbance coefficient. 2) Porphyrin dyes have been demonstrated to possess charge-transfer kinetics indistinguishable from those of ruthenium polypyridyl complexes. 3) Metal porphyryns undergo facile reduction and oxidation, so their optical, photophysical, and electrochemical properties can be systematically tailored by the substitutions and inner metal complexations, by taking advantage of their multiple reactive sites, including four meso and eight β -positions. Elongation of strong electron-donating and electron-withdrawing groups can shift and broaden the absorption range of porphyryns making it possible to increase the light-harvesting property and the resulting DSSC efficiency. The optical, photophysical, and electrochemical properties of the porphyrin can be tuned through functional groups or substitution at their meso and β position. The most efficient porphyrin sensitizers consist of electron donor (D) and electron acceptor (A) groups,

connected via p-conjugated spacers, with the highest achieved power conversion efficiency in DSSCs (13%). Most of these D–p–A structured porphyrin sensitizers contain dialkylamine or diarylamine units as donor groups and ethynyl benzoic acid moieties as acceptors, which are covalently linked to the macrocyclic core. In recent years, perovskite solar cells (PSCs) have become an attractive research area because of their high cell performance. The drawbacks of the high cost of hole-transporting materials, instability of devices and environmentally dangerous lead based materials limit the application of perovskite photovoltaics in the very good future. In this regard, dye-sensitized solar cells based on porphyrin photosensitizers and less harmful iodide– triiodide electrolytes offer a compromising solution to energy conversion in ambient environments. Zn Porphyrin appears to be an essential requirement to develop relatively simple and cost-effective dyes for practical encapsulation of DSSCs into end products for the community. That is, the molecular design of sensitizers should be a trade-off between large scale synthesis and device efficiency. Among the alternative dyes, porphyrins have attracted a great deal of attention because of their strong Soret (400–450 nm) and moderate Q-bands (550–600 nm) absorption properties as well as their natural role in photosynthesis [17]. Furthermore, the photo-chemical and electrochemical stabilities, easy synthetic process and handy control of redox potential by metallisation also make them as promising candidates for light harvesting dyes for DSSC [18-28]. Porphyrins showed highest performance (13%) compared to other dyes in DSSC [29]. The practical application of commercially available (Ruthenium-based) dyes is obstructed by limited resources and high cost of ruthenium metal. Ruthenium based dyes contain lengthy purification process, environmental issues and lower molar extinction coefficients but Zn-Porphyrin based dyes are abundant, easily tuneable structure, the Q band and Moderate band reveals the strong absorption spectrum in the Uv-Vis NIR spectral regions, higher molar extinction coefficients

and better efficiency so the scientific community is looking forward to Zn-Porphyrin based research.

In this study we have synthesized two D- π -A Zn- porphyrin (**SKPor-1** and **SKPor-2**) sensitizers containing same electron withdrawing moiety (carboxylic acid), same metal centre (Zn) and we have modified donor groups such as dimethylaminophenyl, thiophene and we compare the effect of dimethylaminophenyl, thiophene donor groups on the UV-Vis NIR absorption spectrum, Cyclic voltammetry and Photovoltaic performance of the corresponding DSSCs.

2. Experimental Section

2.1. Materials and Reagents

All starting materials were purchased from Sigma Aldrich and Merck. Methyl 4-formylbenzoate, pyrrole, InCl₃, 4-(dimethylamino)benzaldehyde, p-chloranil, Et₃N, Zn (OAc)₂ · 2H₂O, KOH, HCl, thiophenealdehyde, methanol, hexane, chloroform, dimethylformamide, all chemicals and solvents used in this work were of analytical grade and used without further purification. All chromatographic separations were carried out on silica gel (120–160 mesh).

2.2. Analytical Methods

¹H NMR and ¹³C NMR spectra of all the synthesized compounds were recorded in DMSO-d₆ on a Bruker AV III 500 MHz FT NMR spectrometer. The electronic spectra of the dyes with solvent are recorded on a Perkin-Elmer Lambda 35 UV-Vis NIR spectrophotometer. Cyclic voltammetry was carried out with a Versa STAT3 (AMETEK). A three-electrode system consisting of a reference electrode (Ag/AgCl), a working electrode (GC), and a counter electrode (platinum) was used. The redox potential of dyes was measured in DMF with 0.1 M TBAPF₆ with a scan rate of 100 mV s⁻¹.

2.3. Solar Cell Fabrication

Fluorine doped SnO₂ conducting glass (FTO 15Ω/cm²) was washed with isopropanol, ethanol and deionized water using ultrasonic bath for 30 minutes. The FTO glass was treated with 40 mM TiCl₄ aqueous solution at 70 °C for 40 minutes and then the substrates were sintered at 450 °C for 30 minutes in air. The TiO₂ nanoparticles (Degussa P25 Solaronix) was ground for appropriate hours with the Triton X 100, acetyl acetone, ethanol and water to make colloid blend. The 10 μm thick film of TiO₂ nanoparticles was deposited onto the side of conducting layer of FTO by doctor blade technique. TiO₂ substrates were sintered at 450 °C for 30 minutes in air and then immersed in 40 mM TiCl₄ aqueous solution at 70 °C for 40 minutes and then the substrates were sintered at 450 °C for 30 minutes in air. After cooling to 80 °C the TiO₂ electrodes were immersed into 0.5 mM dye solution in ethyl acetate and left for 24 h at room temperature. After dye adsorption, the dye coated TiO₂ electrodes were copiously rinsed with ethanol. Pt (Platisol solaronix) was deposited onto the side of conducting layer of another FTO by doctor blading as the counter electrode and then the substrates were sintered at 450 °C for 30 min in air. The photovoltaic measurements were performed in a sandwich cell consisting of the porphyrin dyes sensitized TiO₂ electrode as the working electrode and Pt as the counter electrode. The electrolyte consists of I⁻/I³⁻ (Iodolyte Solaronix) redox potential and the efficient irradiated area of cell was 0.5 cm x 0.5 cm. The photocurrent – voltage (J–V) characteristics were measured with Oriel Class-AAA Simulator (Newport) with a xenon lamp as a light source having an intensity of 100 mW/cm². Prior to experiment the light intensity was adjusted with a standard PV reference cell (2 cm x 2 cm monocrystalline silicon solar cell, calibrated at NREL, Colorado, USA) with a Keithley 2400 source-measure unit. All photovoltaic properties such as open circuit voltage (V_{oc}), short

circuit current density (J_{sc}), fill factor (FF) obtained from the J-V curve were used in the following equation to obtain power conversion efficiency.

$$\eta = \frac{J_{sc} \text{ (mAcm}^{-2}\text{)} \times V_{oc} \text{ (V)} \times FF}{P_{in} \text{ (mW cm}^{-2}\text{)}}$$

2.4. Synthesis

The synthesis routes of the two porphyrins are shown in Fig. 1. The detailed synthesis procedure is as follows.

2.4.1. Synthesis of 5-(4-Carbomethoxyphenyl) dipyrromethane

The reaction was made by methyl 4-formylbenzoate (1 mmol) and pyrrole (2 mmol) in the presence of InCl_3 (0.1 mmol) taken in round bottom flask and stirred 3 hr at room temperature. Purple colour solid was formed which was purified by column chromatography Methanol: Hexane (10:90) as the eluent. $^1\text{H NMR}$ (300 MHz, DMSO-d_6) δ (ppm): 3.01 (s, 3H, OCH_3), 3.44 (s, 1H, Meso-H), 3.99 (m, 2H, Pyrrolic- $2\text{C}_3\text{-H}$), 4.03 (d, $J = 3.6$ Hz, 2H, Pyrrolic- $2\text{C}_4\text{H}$), 4.83 (m, 2H, Pyrrolic- $2\text{C}_5\text{-H}$), 7.81, (d, $J = 7.4$ Hz, 2H, aromatic- H), 7.47, (d, $J = 7.8$ Hz, 2H, aromatic-H), 8.10, (s, 2H, 2N-H). $^{13}\text{C NMR}$ (400 MHz, DMSO-d_6); δ (ppm) 40.12, 45.09, 76.84, 77.15, 77.48, 111.07, 115.42, 118.34, 162.20, 162.35. GC-MS: m/z calculated for $[\text{C}_{17}\text{H}_{16}\text{N}_2\text{O}_2 + \text{H}]^+$ 280.3211. Found: 280.2127 $[\text{M} + \text{H}]^+$.

2.4.2. Formation of Porphyrin Ring

Solution of 4-(dimethylamino)benzaldehyde (2 mmol) and 5-(4-carbomethoxyphenyl)dipyrromethane (2 mmol) in 250 mL of chloroform was passed with argon gas for 40 minutes. Trifluoroacetic acid (2 mmol) was added and the obtained solution was stirred in the dark at nitrogen atmosphere for 18 hr. Finally the para-chloranil (6 mmol) was added and stirred for 3 hr. Triethylnitrate (2 mL) was added to complete the reaction. The solvent was evaporated and the mixture was passed through TLC silica to remove the

non-porphyrin products and then the purification was done by column chromatography using dichloromethane: ethyl acetate (95: 5) as an eluent to give the porphyrin as a pure product. ^1H NMR (300 MHz, CDCl_3) δ (ppm): 8.90 (d, $J=5.4$ Hz, 4H, Aromatic H), 8.77 (d, $J=7.5$ Hz, 4H, Aromatic H), 8.48 (d, $J=7.5$ Hz, 4H, Pyrrolic H), 8.36 (d, $J=7.5$ Hz, 4H, Pyrrolic H), 8 (d, $J=9.2$ Hz, 4H, Aromatic H), 6.7 (d, $J=9.2$ Hz, 4H, Aromatic H), 4.28 (s, 6H, COOMe), 4.12 (s, 12H, NMe_2), 1.07 (s, 2H, Porphyrin NH). ^{13}C NMR (300 MHz, CDCl_3); δ (ppm) 153.2, 151.6, 151.2, 150.7, 145.8, 145.3, 143.6, 142.1, 140.8, 139.9, 133.7, 133.4, 131.8, 131.4, 131.1, 127.5, 127.2, 126.3, 113.9, 112.7, 29.8. GC-MS: m/z calculated for $[\text{C}_{44}\text{H}_{30}\text{N}_2\text{O}_4\text{S}_2 + \text{H}]^+$ 742.8634. Found: 742.8623 $[\text{M}+\text{H}]^+$.

2.4.3. Metallisation of Zn-Porphyrin (SKPor-1)

The solution of **2.4.2.** (1 mmol) in 15 mL of CHCl_3 , a methanol solution of zinc acetate dehydrate (1.5 mmol) was added and the solution was refluxed under nitrogen atmosphere for 8 hr. The solvent was evaporated, the residue was washed with distilled water (20 mL). The solution (0.5 mmol) with 25 mL of tetrahydrofuran– methanol (1: 1) mixture was added to 10 mL of aqueous KOH (1 mmol) solution and refluxed for 46 hr. Then the solvent was evaporated and the resulting residue was added to 10 mL of distilled water. HCl solution was added to the precipitation of the porphyrin, which was filtered and washed with water and then dried under vacuum to give the final product as a purple **SKPor-1.** ^1H NMR (400 MHz, $\text{DMSO}-d_6$) δ (ppm): 11.9 (s, 2H, COOH), 9.79 (s, 4H, Porphyrin Pyrrolic H), 7.89 (s, 4H, Porphyrin Pyrrolic H), 7.66 (d, $J=8.8$ Hz, 8H, Aromatic H), 7.31 (d, $J=8$ Hz, 4H, Aromatic H), 7.07 (d, $J=8$ Hz, 4H, Aromatic H), 2.76 (s, 12H, NMe_2). ^{13}C NMR (400 MHz, $\text{DMSO}-d_6$); δ (ppm) 190.44, 153.40, 147.90, 146.21, 131.33, 129.77, 129.50, 129.23, 129.17, 128.94, 126.35, 125.15, 124.20, 122.81, 122.70, 119.40, 35.46. GC-MS: m/z calculated for $[\text{C}_{42}\text{H}_{24}\text{N}_4\text{O}_4\text{S}_2\text{Zn} + \text{H}]^+$ 778.1743. Found: 778.1758 $[\text{M}+\text{H}]^+$.

2.4.4. Formation of Porphyrin Ring

The solution of 2-thiophenecarboxyaldehyde (2 mmol) and 5-(4-carbomethoxyphenyl)dipyrromethane (2 mmol) in 250 mL of chloroform was passed with argon gas for 40 minutes. Trifluoroacetic acid (2 mmol) was added and the obtained solution was stirred in the dark at nitrogen atmosphere for 18 hr. Finally the para-chloranil (6 mmol) was added and stirred for 3 hr. Triethylnitrate (2 mL) was added to complete the reaction. The solvent was evaporated and the mixture was passed through TLC silica to remove the non-porphyrin products and then the purification was done by column chromatography using dichloromethane: ethyl acetate (95: 5) as an eluent to give the porphyrin as a pure product. ^1H NMR (300 MHz, CDCl_3) δ (ppm): 8.78 (d, $J=9.2$ Hz, 4H, Porphyrin Pyrrolic H), 8.46 (d, $J=9.2$ Hz, 4H, Porphyrin Pyrrolic H), 8.32 (d, $J=8.4$ Hz, 4H, Aromatic H), 8.18 (d, $J=8.4$ Hz, 4H, Aromatic H), 7.87 (d, $J=9.4$ Hz, 2H, Thienyl H), 7.42 (s, 4H, Thienyl H), 5.32 (s, 6H, COOMe), 3.89 (s, 12H, NMe_2), 0.80 (s, 2H, Porphyrin NH). ^{13}C NMR (300 MHz, CDCl_3); δ (ppm) 158.8, 149.8, 148.3, 141.6, 132.3, 129.9, 128.4, 128.1, 127.8, 127.5, 126.3, 125.7, 124.6, 121.9, 121.4, 117.8, 36.2. GC-MS: m/z calculated for $[\text{C}_{52} \text{H}_{44} \text{N}_6 \text{O}_4 + \text{H}]^+$ 817.3502. Found: 817.3289 $[\text{M}+\text{H}]^+$.

2.4.5. Metallisation of Zn-Porphyrin (SKPor-2)

The solution of **2.4.4.** (1 mmol) in 15 mL of CHCl_3 , a methanol solution of zinc acetate dehydrate (1.5 mmol) was added and the solution was refluxed under nitrogen atmosphere for 8 hr. The solvent was evaporated, the residue was washed with distilled water (20 mL). The solution (0.5 mmol) with 25 mL of tetrahydrofuran– methanol (1: 1) mixture was added to 10 mL of aqueous KOH (1 mmol) solution and refluxed for 46 hr. Then the solvent was evaporated and the resulting residue was added to 10 mL of distilled water. HCl solution was added to the precipitation of the porphyrin, which was filtered and washed with water and then dried under vacuum to give the final product as a purple **SKPor-2.** ^1H NMR

(400 MHz, DMSO-d₆) δ (ppm): 12.7 (s, 2H, COOH), 7.92 (s, 4H, Porphyrin Pyrrolic H), 7.90 (s, 4H, Porphyrin Pyrrolic H), 7.88 (d, J=8.4 Hz, 4H, Aromatic H), 7.18 (d, J=8.8 Hz, 4H, Aromatic H), 6.67 (d, J= 6.8 Hz, 4H, Thienyl H), 6.10 (s, 4H, Thienyl H). ¹³C NMR (400 MHz, DMSO-d₆); δ (ppm) 178.6, 167.1, 147.6, 132, 131.8, 129.9, 128.7, 128.4, 118.5, 117.6, 108.4, 107.7, 106.1. GC-MS: m/z calculated for [C₅₀ H₃₈ N₆ O₄ Zn + H]⁺ 851.2324. Found: 851.2345 [M+H]⁺.

3. Results and Discussions:

3.1 Absorption Spectrum

The Zn-porphyrin dye exhibits the typical features of a porphyrin ring that is an intense Soret band in the range 350–450 nm and a less intense Q band in the range 450–700 nm. The UV–vis NIR absorption spectra of the **SKPor-1** and **SKPor-2** dyes in DMF solution are shown in Fig. 2. The peak positions and molar absorption coefficients (ϵ) of Soret and Q-bands of **SKPor-1** and **SKPor-2** dyes are listed in Table.1. The UV–vis NIR absorption spectra of **SKPor-1** dye exhibits a strong Soret band at 381 nm and two moderate Q-bands at 483 and 650 nm and **SKPor-2** dye exhibits a strong Soret band at 374 nm and two moderate Q-bands at 476 and 619 nm. The strong intense Soret band of both dyes between 350 nm to 435 nm are due to intermolecular π - π^* electronic transition and the porphyrin species consist of a strong transition to the second excited state (S_0 - S_2). The broad less intense second Q-bands of both dyes between 450 nm to 675 nm are due the intermolecular n- π^* electronic transition and this involves weak transition to the first excited state (S_0 - S_1). However, the strong Soret band and moderate Q-bands of **SKPor-1** are broader and red- shifted than that of **SKPor-2**. The absorption spectrum of **SKPor-1** the Soret band and the first Q-bands are red-shifted around 10 nm and the second Q-band is red shifted around 30 nm than **SKPor-2**. This is because **SKPor-1** contains dimethylaminophenyl group at meso-position which have

more phenyl-conjugated double bonds and more electron withdrawing nature compared to thienyl group of **SKPor-2** [30-31]. The molar extinction coefficients (ϵ) of **SKPor-1** Soret band $2.08 \times 10^5 \text{ mol L}^{-1} \text{ cm}^{-1}$, first Q-band is $0.42 \times 10^5 \text{ mol L}^{-1} \text{ cm}^{-1}$, second Q-band is $0.45 \times 10^5 \text{ mol L}^{-1} \text{ cm}^{-1}$. For **SKPor-2** dye Soret band $1.68 \times 10^5 \text{ mol L}^{-1} \text{ cm}^{-1}$, first Q-band is $0.29 \times 10^5 \text{ mol L}^{-1} \text{ cm}^{-1}$, second Q-band is $0.21 \times 10^5 \text{ mol L}^{-1} \text{ cm}^{-1}$ which are lower than that of **SKPor-1**. As a consequence of an extended π -conjugation, both Soret and Q bands of **SKPor-1** exhibit a significant red shift and a Soret band broader than that of **SKPor-2**, because the electronic interaction with the dimethylaminophenyl group is more pronounced than for the thienyl group. The results clearly show that more π -conjugation with a highly conjugated phenyl bridge unit can improve the light-harvesting capability of Zn-porphyrin dyes. These results indicate that the **SKPor-1** has more light harvesting ability compared to **SKPor-2**.

3.2. Cyclic Voltammetry

The electrochemical studies are performed on the **SKPor-1** and **SKPor-2** dyes to elucidate the oxidation and reduction potentials corresponding to the HOMO energy level and LUMO energy level of the dyes via cyclic voltammetry. The cyclic voltammetry measurements for **SKPor-1** and **SKPor-2** in DMF were conducted using tetrabutylammonium hexafluorophosphate (TBAPF₆, 0.1 M) as supporting electrolyte at scan rate of 100 mV/s with three electrode system. The potentials are listed in table.2. All potentials are quoted with respect to a non-aqueous silver/silver chloride (Ag/AgCl) reference electrode, this electrode was externally calibrated with the Fc/Fc⁺ redox couple in the dimethylformamide solution and has a potential of 0.552 V versus NHE. **SKPor-1** contains three successive quasi-reversible redox couples with the first anodic and cathodic peak potentials -0.72 V, -0.85 V; the second anodic and cathodic peak potentials 0.17 V, 0.11 V;

and the third anodic and cathodic peak potentials 1.14 V, 1.00 V respectively. The HOMO value of the **SKPor-1** is -5.79 eV which was calculated using the oxidation potential 1.14 V. The LUMO value is -3.03 eV which was estimated from the HOMO energy value with the intersection point of absorption spectrum. **SKPor-2** contains two successive quasi-reversible redox couples with the first anodic and cathodic peak potentials 1.24 V, -0.32 V and the second anodic and cathodic peak potentials 1.49 V, -0.88 V respectively which is shown in Fig.3. The HOMO value of the **SKPor-2** is -6.09 eV which was calculated using the oxidation potential 1.49 V. The LUMO value is -3.20 eV which was estimated from the HOMO energy value with the intersection point of absorption spectrum. In addition, with the introduction of the stronger donor group, the energy levels of HOMO and LUMO are largely changed. To ensure efficient electron injection from the LUMO of the sensitizer into the conduction band of TiO₂, the LUMO level must be higher than the conduction band edge of TiO₂. The HOMO level of the sensitizer must be lower than the redox potential of I⁻/I³⁻ electrolyte for efficient regeneration of the sensitizer cations after the photo-induced electron injection into the conduction band of TiO₂ [32-35]. The resulted HOMO value of the **SKPor-1** is -5.79 eV which is lower than the redox potential of I⁻/I³⁻ value (-4.94 eV) and LUMO value is -3.03 eV which is higher than the conduction band value of TiO₂ (-4.04 eV) so this provides enough driving force to inject electrons from the excited **SKPor-1** singlet state to the conduction band of TiO₂.

SKPor-1 and **SKPor-2** dyes have been fully optimized with B3LYP/6-311g (d,p) level of theory without any symmetry constraints. The vibrational frequency calculations were performed at the same level of theory to ensure that the **SKPor-1** and **SKPor-2** structures are true minima (no imaginary frequencies) on the potential energy surface. Fig. 4 shows the optimized molecular structure of **SKPor-1** and **SKPor-2** dye molecules. All calculations were performed using Gaussian 09 W programme package [36]. The ground-

state geometries and electronic properties such as highest occupied molecular orbital (HOMO) and lowest unoccupied molecular orbital (LUMO) energy densities were calculated at B3LYP/6-311g (d,p) level basis set. The frontier molecular orbital (FMO) plays a vital role in the charge separated states of organic molecules. The HOMO and LUMO energies of dye sensitizers have suitable energy values for matching the conduction band edge of semiconductor and redox potential of electrolyte in DSSCs. In DSSC, HOMOs are delocalized over the donor part and LUMOs are delocalized over the acceptor part and anchoring group of dye molecules. Fig. 5 shows the FMOs of **SKPor-1** and **SKPor-2** dyes. From Fig. 5 we see that the electron densities for **SKPor-1** and **SKPor-2** HOMO-2 are delocalized over the donor part, HOMO-1 is delocalized on porphyrin core and HOMO is delocalized on porphyrin unit and donor part of the molecule. While the LUMO is delocalized in porphyrin core unit and smaller electron densities are delocalized in acceptor part, LUMO+1 are delocalized on porphyrin core and LUMO+2 delocalized on acceptor part and anchoring group of the molecule. The FMOs analysis gives the clue for charge density transfer in the dye molecule.

3.3. Photovoltaic Performance of the **SKPor-1** and **SKPor-2**.

Liyang Luo, et al. and Ram Ambre, et al. have reported thienyl donor group based Zn-Porphyrins. They achieved solar cell efficiency of 1.8% and 0.8% [37-38]. In order to study the influence of different donor units of Zn-Porphyrin (**SKPor-1** and **SKPor-2**) on the DSSC device performance, photovoltaic experiments were conducted. The devices were assembled using TiO₂ (Degussa P25 Solaronix) film (10 μ m) in conjugation with commercially available N719 dye, synthesized dyes (**SKPor-1** and **SKPor-2**), I/I³⁻ (Iodolyte Solaronix) based electrolyte and Pt as cathode. Fig. 5 shows the photocurrent-voltage (J_{sc}-V) characteristics of DSSC devices sensitized by **SKPor-1** and **SKPor-2** under standard air mass 1.5 global spectral solar photon flux. The short-circuit photocurrent density (J_{sc}), open-circuit voltage

(Voc) and fill factor (FF) of the two devices are summarized in Table. 4. The overall power conversion efficiency (PCE) of DSSC devices stained with dyes **SKPor-1** and **SKPor-2** was 3.2 % and 2.5 %, respectively. This implies the enhancement of the photo-induced charge collection of **SKPor-1** sensitized devices over **SKPor-2** devices in association with the standard Γ/I^{3-} based redox electrolyte. It can be concluded from these preliminary results that the DSSCs sensitized with **SKPor-1** bearing the electron donating dimethylaminophenyl core unit, achieved better photovoltaic performance than those sensitized with **SKPor-2** engaging the electron donating thienyl core unit. The higher power conversion efficiency of the **SKPor-1** based DSSCs compared with that of the **SKPor-2** based DSSCs was mainly due to high J_{sc} that is attributed to the excessive conjugated double bonds of the dimethylaminophenyl core unit possibly enhancing the efficiency, regeneration of electrons and also increasing electron injection from the **SKPor-1** molecules to TiO_2 . The poor PCE of the **SKPor-2** DSSCs may be resulted from their unfavorable orientation due to the lower conjugation of the molecules and the aggregation of the Zn-porphyrin macrocycles.

3.4. Dye Adsorption measurement of the **SKPor-1**, **SKPor-2** and **N719** Dyes.

In order to find out the amount of dye molecule adsorbed on the TiO_2 surface we prepared 0.5 mM of dye (**SKPor-1**, **SKPor-2** and **N719** dyes) solutions, then analyzed with the UV-Vis NIR spectrum. The results are shown in Fig.7. Using these absorption values the molar extinction coefficient of the initial dye solution was calculated through Beer- Lamberts law. TiO_2 films were immersed into the same dye solutions for 24 hrs, after that TiO_2 films were taken out. Dye desorption was carried out by 0.5 mM of NaOH in a mixed solvent (water: ethanol = 1:1, v: v for **N719**, water: DMF = 1:9, v: v for **SKPor-1** and **SKPor-2**). Then, UV-Vis absorption spectra of the resultant solutions were measured to estimate the amount of adsorbed dye molecules [39-42]. The results are shown in Fig.8. **SKPor-1**,

SKPor-2 and **N719** dye molecules adsorbed onto the TiO_2 surface are $8.1 \times 10^{-8} \text{M Cm}^{-2}$, $2.3 \times 10^{-8} \text{M Cm}^{-2}$ and $2.8 \times 10^{-8} \text{M Cm}^{-2}$, respectively, The results are shown in Table. 5.

4. Conclusion

In conclusion, **SKPor-1** sensitizer cell gave J_{SC} of 9.62 mA cm^{-2} , V_{OC} of 0.68 V , and FF of 0.50 , corresponding to an overall conversion efficiency of **3.2 %** because of a bulky donor effect. **SKPor-2** sensitizer cell gave J_{SC} of 7.2 mA cm^{-2} , V_{OC} of 0.68 V , and FF of 0.51 , corresponding to an overall conversion efficiency of **2.5 %**. Zn-porphyrin with dimethylaminophenyl moiety (**SKPor-1**) showed a higher conversion efficiency because it contains **strong and wide absorption spectrum in the Uv-Vis NIR spectral regions**, so **corresponding molar extinction coefficients have increased ($2.08 \times 10^5 \text{ mol L}^{-1} \text{ cm}^{-1}$) compared to SKPor-2 dye ($1.68 \times 10^5 \text{ mol L}^{-1} \text{ cm}^{-1}$)**. Cyclic voltammetry results show the **HOMO and LUMO energy levels of the SKPor-1 dye as -5.79 eV and -3.03 eV , respectively. The HOMO and LUMO energy levels of the SKPor-2 dye are -6.09 eV and -3.20 eV , respectively. The HOMO value of the SKPor-1 is -5.79 eV which is lower than the redox potential of I^-/I^{3-} value (-4.94 eV) and LUMO value is -3.03 eV which is higher than the conduction band value of TiO_2 (-4.04 eV) so this provides enough driving force to inject electrons from the excited SKPor-1 singlet state to the conduction band of TiO_2 compared to SKPor-2. The amount of SKPor-1 dye adsorbed on semiconductor surface is $81 \times 10^{-8} \text{M Cm}^{-2}$ and the amount of SKPor-2 dye adsorbed on semiconductor surface is $23 \times 10^{-8} \text{M Cm}^{-2}$. Compared to SKPor-2 dye, SKPor-1 dye is adsorbed more so SKPor-1 based solar cell gives higher efficiency. Compared to SKPor-1 and SKPor-2 dyes, commercially available N719 dye is having wide absorption and appropriate HOMO-LUMO values resulting in higher efficiency. Further improvement of the power**

conversion efficiency of Zn-porphyrin derivative dyes can be investigated by using them as dye sensitizers instead of expensive ruthenium dye sensitizers in the near future.

Acknowledgements

The authors thank SIF, VIT, Vellore for NMR analysis, SAIF, IIT, Madras for providing Mass spectrometry analysis and we also thank DST (SERI) DST/TM/SERI/2k12/40(G) & 04.06.2014 for financial support.

References

1. B. Oregan, M. Gratzel, *Nature* 353 (1991) 737-740.
2. A. Mishra, M.K.R. Fischer, P. Bauerle, *Angew. Chem. Int. Ed.* 48 (2009) 2474-2499.
3. W.M. Campbell, A.K. Burrell, D.L. Officer, K.W. Jolley, *Coord. Chem. Rev.* 248 (2004) 1363-1379.
4. Cheng-Wei Lee, Hsueh-Pei Lu Nagannagari Masi Reddy , Hsuan-Wei Lee , Eric Wei-Guang Diao, Chen-Yu Yeh. *Dyes and Pigments* 91 (2011) 317-323.
5. Kalyan Kumar Pasunooti, Jun-Ling Song, Hua Chai, Pitchamuthu Amaladass, Wei-Qiao Deng, Xue-Wei Liu. *Journal of Photochemistry and Photobiology A: Chemistry* 218 (2011) 219-225.
6. Dimitra Daphnomili, G.D. Sharma, S. Biswas, K.R. Justin Thomas, A.G. Coutsolelos. *Journal of Photochemistry and Photobiology A: Chemistry* 253 (2013) 88-96.
7. L. Moreira Goncalves, V. de Zea Bermudez, A. Ribeiro, A. Magaltes Mendes, *Energy and Environmental Science* 1 (2008) 655.

8. Wang Q, Campbell WM, Bonfantani EE, Jolley KW, Officer DL, Walsh PJ, et al. *Journal of Physical Chemistry B* 109 (2005) 15397-15409.
9. Hagfeldt A, Gratzel M. Molecular photovoltaics. *Accounts of Chemical Research* 33 (2000) 269-277.
10. Gratzel M. et al. *Inorganic Chemistry* 44 (2005) 6841-6851.
11. Robertson N. et al. *Angewandte Chemie International Edition* 45 (2006) 2338-2345.
12. Tachibana Y, Haque SA, Mercer IP, Durrant JR, Klug DR. *Journal of Physical Chemistry B* 104 (2000) 1198-1205.
13. Nazeeruddin MK, Angelis DF, Fantacci S, Selloni A, Viscardi G, Liska P, et al. *Journal of American Chemical Society* 127 (2005) 16835-16847.
14. Wang P, Klein C, Moser JE, Baker RH, Ha NLC, Charvet R, et al. *Journal of Physical Chemistry B* 108 (2004) 17553-17559.
15. Gratzel M. et al. *Photochemistry Reviews* 4 (2003) 145-153.
16. Na Xiang, Xianwei Huang, Xiaoming Feng, Yijiang Liu, Bin Zhao, Lijun Deng, Ping Shen, Junjie Fei, Songting Tan. *Dyes and Pigments* 88 (2011) 75-83.
17. W.M. Campbell, K.W. Jolley, P. Wagner, K. Wagner, P.J. Walsh, K.C. Gordon, L. Schmidt-Mende, M.K. Nazeeruddin, Q. Wang, M. Gratzel, D.L. Officer, J. Phys. Chem. C. 111 (2007) 11760-11762.
18. Y. Liu, N. Xiang, X. Feng, P. Shen, W. Zhou, C. Weng, B. Zhao, S.T. Tan, *Chem. Commun.* (2009) 2499-2501.
19. M. Tanaka, S. Hayashi, S. Eu, T. Umeyama, Y. Matano, H. Imahori, *Chem. Commun.* 20 (2007) 2069-2071.

20. M.K. Nazeeruddin, R. Humphry-Baker, D.L. Officer, W.M. Campbell, A.K. Burrell, M. Gratzel, *Langmuir* 20 (2004) 6514-6517.
21. H. Imahori, S. Hayashi, H. Hayashi, A. Oguro, S. Eu, T. Umeyama, Y. Matano, J. *Phys. Chem. C* 113 (2009) 18406-18413.
22. S. Hayashi, M. Tanaka, H. Hayashi, S. Eu, T. Umeyama, Y. Matano, Y. Araki, H. Imahori, J. *Phys. Chem. C* 112 (2008) 15576-15585.
23. W.M. Campbell, K.W. Jolley, P. Wagner, K. Wagner, P.J. Walsh, K.C. Gordon, L. Schmidt-Mende, M.K. Nazeeruddin, Q. Wang, M. Gratzel, D.L. Officer, *J. Phys. Chem. C* 111 (2007) 11760-11762.
24. E.E. Bonfantini, A.K. Burrell, W.M. Campbell, M.J. Crossley, J.J. Gosper, M.M. Harding, D.L. Officer, D.C.W. Reid, *J. Porphyrins Phthalocyanines* 6 (2002) 708-719.
25. Q. Wang, W.M. Campbell, E.E. Bonfantini, K.W. Jolley, D.L. Officer, P.J. Walsh, K.Gordon, R. Humphrybaker, M.K. Nazeeruddin, M. Gratzel, D.L. Officer, *J. Phys. Chem. B* 109 (2005) 15397-15409.
26. N.K. Subbaiyan, L. Obraztsov, C.A. Wijesinghe, K. Tran, W. Kutner, F. D'Souza, *J. Phys. Chem. C* 113 (2009) 8982-8989.
27. N. Kristian, Y.L. Yu, P. Gunawan, R. Xu, W.-Q. Deng, X.-W. Liu, X. Wang, *Electrochim. Acta* 54 (2009) 4916-4924.

28. C.W. Lee, H.P. Lu, C.M. Lan, Y.L. Huang, Y.R. Liang, W.N. Yen, Y.C. Liu, Y.S. Lin, E.W.G. Diau, C.Y. Yeh, *Chem. Eur. J.* 15 (2009) 1403–1412.
29. Simon Mathew¹, Aswani Yella¹, Peng Gao¹, Robin Humphry-Baker, Basile F. E. Curchod, Negar Ashari-Astani, Ivano Tavernelli, Ursula Rothlisberger, Md. Khaja Nazeeruddin and Michael Gratzel. *Nature*. 6 (2014) 242-247.
30. Lin CY, Lo CF, Luo L, Lu HP, Hung CS, Diau EWG. *J Phys Chem C* 113 (2009) 755- 764.
31. Kang Deuk Seo , Myung Jun Lee , Hae Min Song , Hong Seok Kang , Hwan Kyu Kim. *Dyes and Pigments* 94 (2012) 143-149.
32. V.V. Pavlishchuk, A.W. Addison, *Inorg. Chim. Acta* 298 (2000) 97-102.
33. D.P. Hagberg, J.-H. Yum, H. Lee, F.D. Angelis, T. Marinado, K.M. Karlsson, R. Humphry-Baker, L. Sun, A. Hagfeldt, M. Grätzel, M.K. Nazeeruddin, *J. Am. Chem. Soc.* 130 (2008) 6259-6266;
34. J.K. Park, H.R. Lee, J. Chen, H. Shinokubo, A. Osuka, D. Kim, *J. Phys. Chem. C* 112 (2008) 16691-16699.
35. Aritat Luechai, Nuttapol Pootrakulchote, Thanisa Kengthanomma, Parichatr Vanalabhatana, Patchanita Thamyongkit. *Journal of Organometallic Chemistry* 753 (2014) 27-33.
36. Gaussian 09, Revision D.01, M. J. Frisch, G. W.Trucks,H.B. Schlegel,G. E. Scuseria,

M. A. Robb, J. R. Cheeseman, G. Scalmani, V. Barone, B. Mennucci, G. A.

Petersson,

H. Nakatsuji, M. Caricato, X. Li, H. P. Hratchian, A. F. Izmaylov, J. Bloino, G. Zheng,

J. L. Sonnenberg, M. Hada, M. Ehara, K. Toyota, R. Fukuda, J. Hasegawa, M. Ishida,

T. Nakajima, Y. Honda, O. Kitao, H. Nakai, T. Vreven, J. A. Montgomery, Jr., J. E.

Peralta, F. Ogliaro, M. Bearpark, J. J. Heyd, E. Brothers, K. N. Kudin, V. N.

Staroverov,

R. Kobayashi, J. Normand, K. Raghavachari, A. Rendell, J. C. Burant, S. S. Iyengar,

J.

Tomasi, M. Cossi, N. Rega, J. M. Millam, M. Klene, J. E. Knox, J. B. Cross, V.

Bakken,

C. Adamo, J. Jaramillo, R. Gomperts, R. E. Stratmann, O. Yazyev, A. J. Austin, R.

Cammi, C. Pomelli, J. W. Ochterski, R. L. Martin, K. Morokuma, V. G. Zakrzewski,

G.

A. Voth, P. Salvador, J. J. Dannenberg, S. Dapprich, A. D. Daniels, Ö. Farkas, J. B.

Foresman, J. V. Ortiz, J. Cioslowski, and D. J. Fox, Gaussian, Inc., Wallingford CT,

2009.

37. Liyang Luo, Ram B. Ambre, Sandeep B. Mane, Eric Wei-Guang Diau and Chen-

Hsiung

Hung, *J. Phys. Chem. Chem. Phys.* (2015), DOI: 10.1039/C5CP02367J.

38. Ram Ambre, Kwan-Bo Chen, Ching-Fa Yao, Liyang Luo, Eric Wei-Guang Diau,

and Chen-Hsiung Hung, *J. Phy. Chem.* 116 (2012), 11907–11916.

39. Inseok Jang, Kyungho Song, Jun-Hwan Park, and Seong-Geun Oh, *Bull. Korean Chem. Soc.* (34) 2013, 2883-2888.
40. Tammy P. Chou, Qifeng Zhang, and Guozhong Cao, *J. Phys. Chem. C*, 111 (2007), 18804-18811.
41. Nansra Heo, Yongseok Jun & Jong Hyeok Park, *Scientific Reports*, 3: 1712, DOI:10.1038/srep01712.
42. N. Shahzada, D. Pugliesea, A. Lamberti, A. Sacco, A. Virga, R. Gaziaa, S. Bianco, M. I. Shahzad, E. Tresso, and C. F. Pirri, *Journal of Physics*: **439** (2013) 012012.

Figures

Figure.1. Synthesis of **SKPor-1** and **SKPor-2**.

Figure.2. UV-Vis NIR spectrum of **SKPor-1** and **SKPor-2**.

Figure.3. Cyclic voltammetry of **SKPor-1** and **SKPor-2** scan rate at 100mV/Sec.

Figure.4. Optimized molecular structures of SKPor-1 and SKPor-2 (For clarity hydrogen atoms are omitted)

Figure.5. Frontier molecular orbitals of **SKPor-1** (top) and **SKPor-2** (bottom)

Figure.6. Current-voltage characteristics of the **SKPor-1**, **SKPor-2** and **N719** dyes.

Figure.7. UV-Vis NIR absorption spectrum of 0.5 mM dye (**SKPor-1**, **SKPor-2** and **N719** dyes) solutions.

Figure.8. UV-Vis NIR absorption spectrum of dye (**SKPor-1**, **SKPor-2** and **N719** dyes) desorbed solutions.

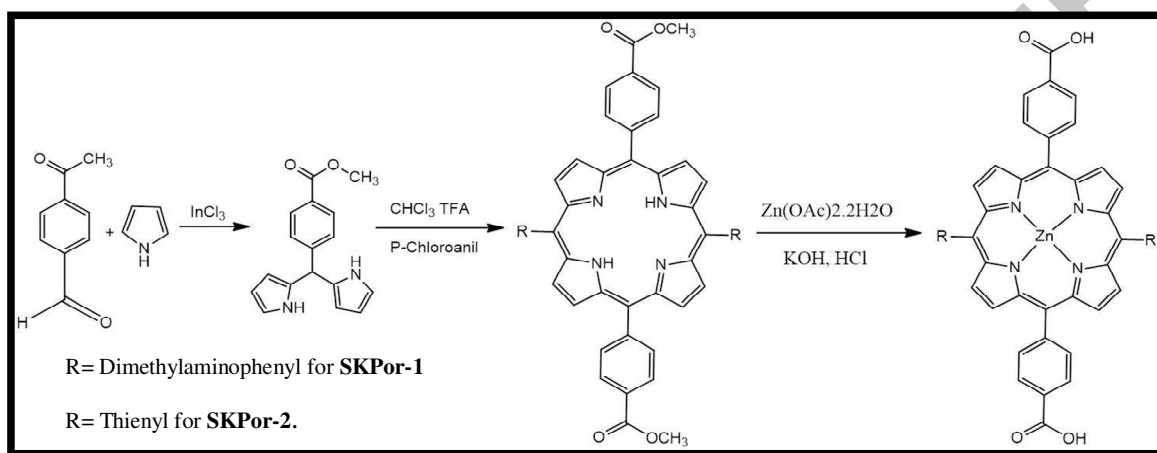
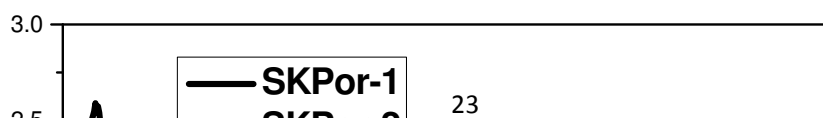


Figure.1. Synthesis of SKPor-1 and SKPor-2.



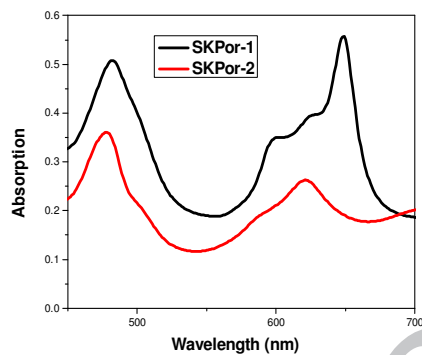


Figure.2. UV-Vis NIR spectrum of SKPor-1 and SKPor-2.

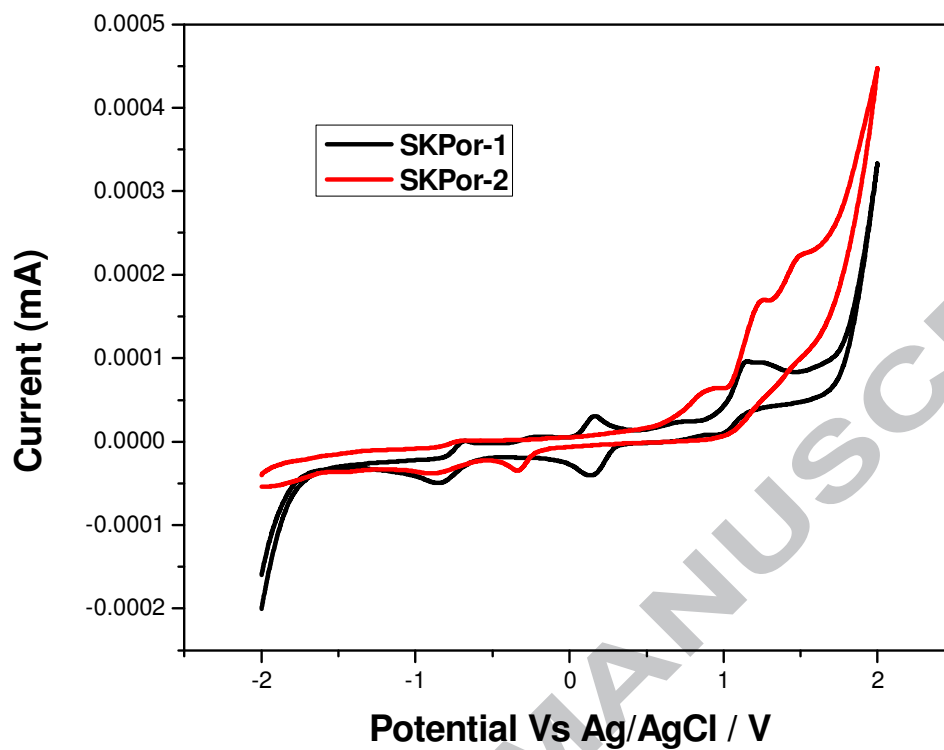


Figure.3. Cyclic voltammetry of SKPor-1 and SKPor-2 scan rate at 100 mV/Sec.

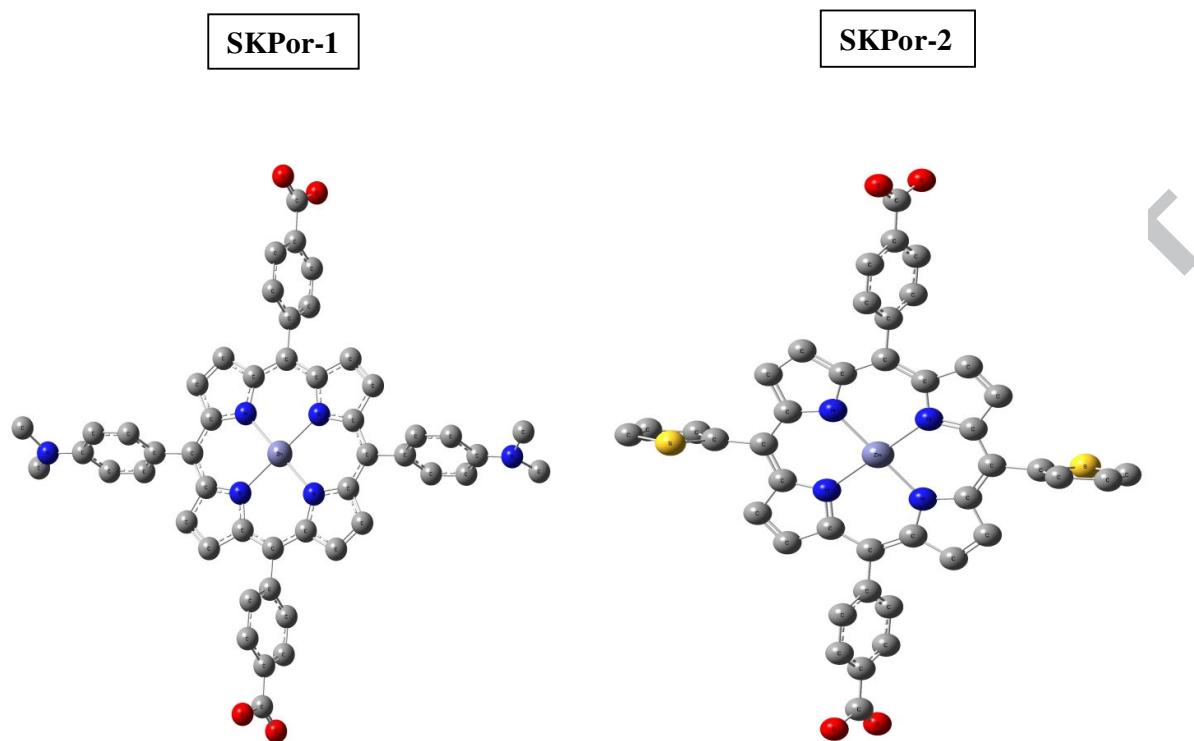


Figure. 4. Optimized molecular structures of SKPor-1 and SKPor-2 (For clarity hydrogen atoms are omitted)

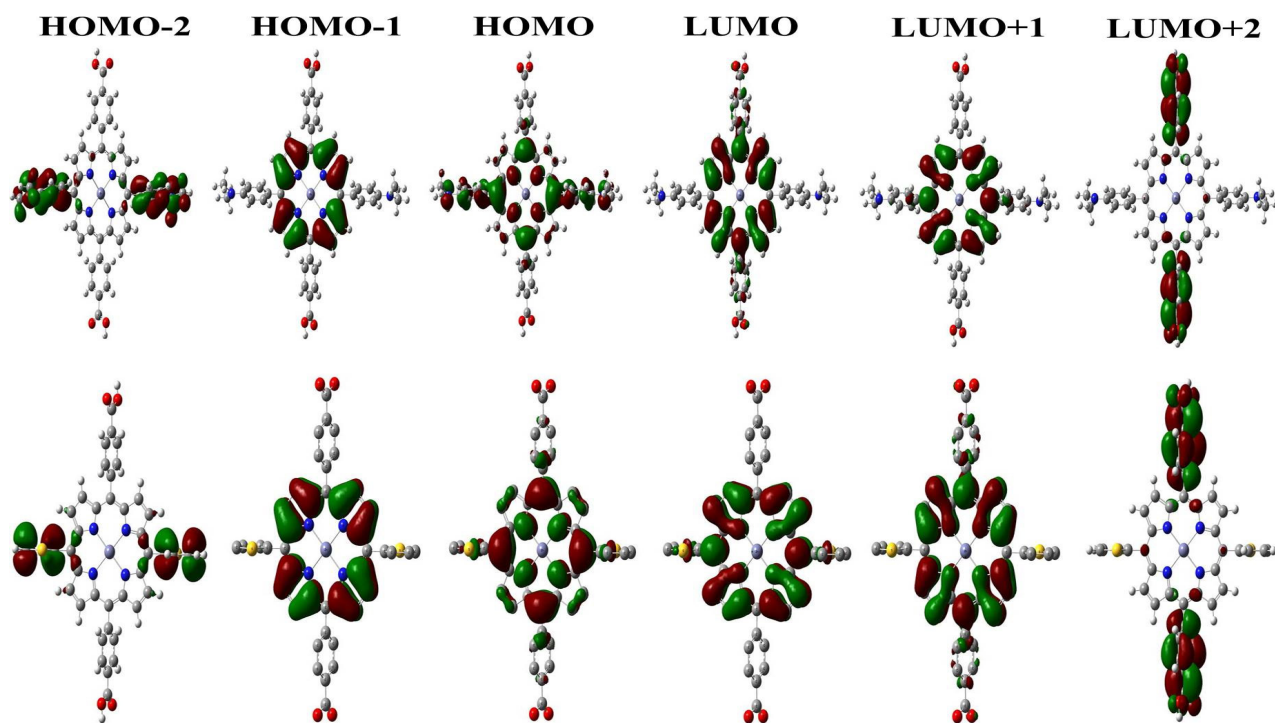


Figure. 5. Frontier molecular orbitals of SKPor-1 (top) and SKPor-2 (bottom)

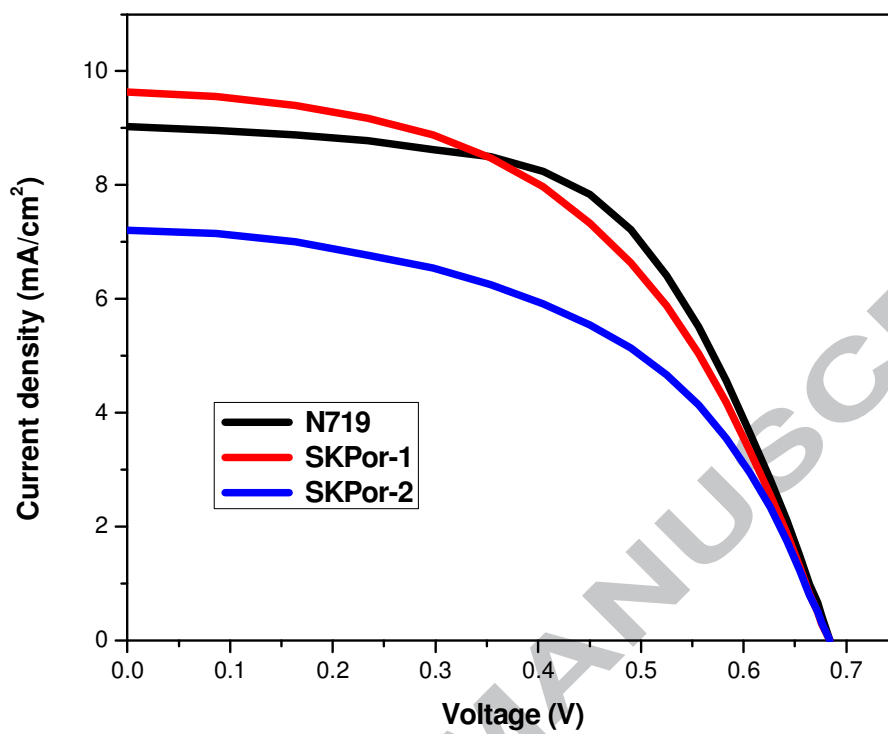


Figure.6. Current-voltage characteristics of the SKPor-1 and SKPor-2 dyes.

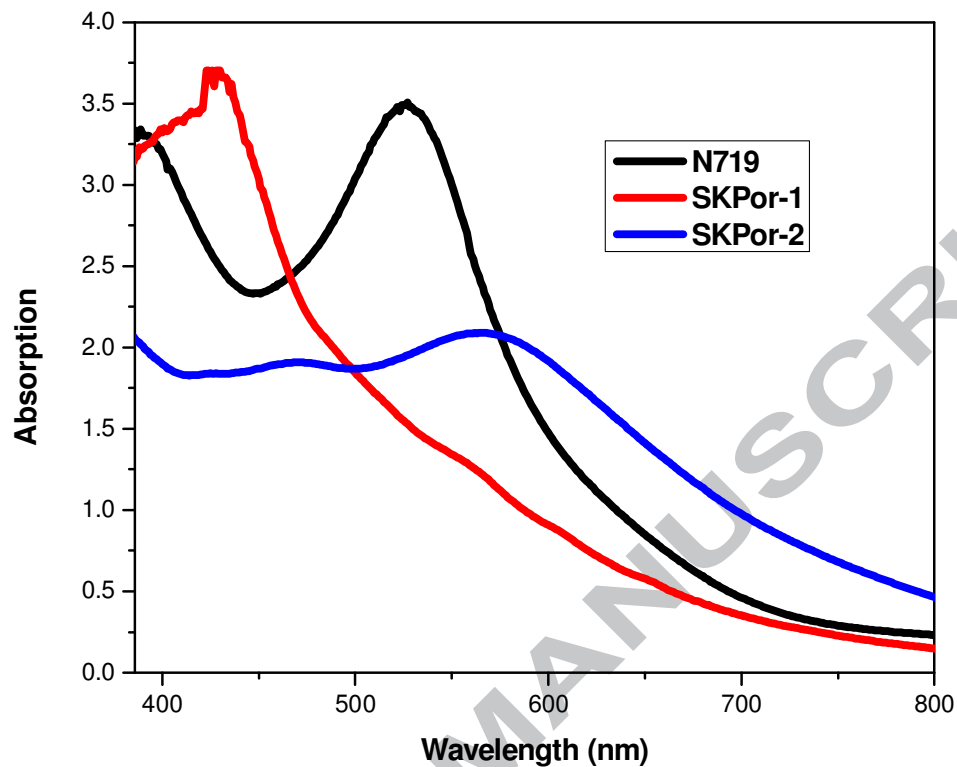


Figure.7. UV-Vis NIR absorption spectrum of 0.5 mM dye (SKPor-1, SKPor-2 and N719 dyes) solutions.

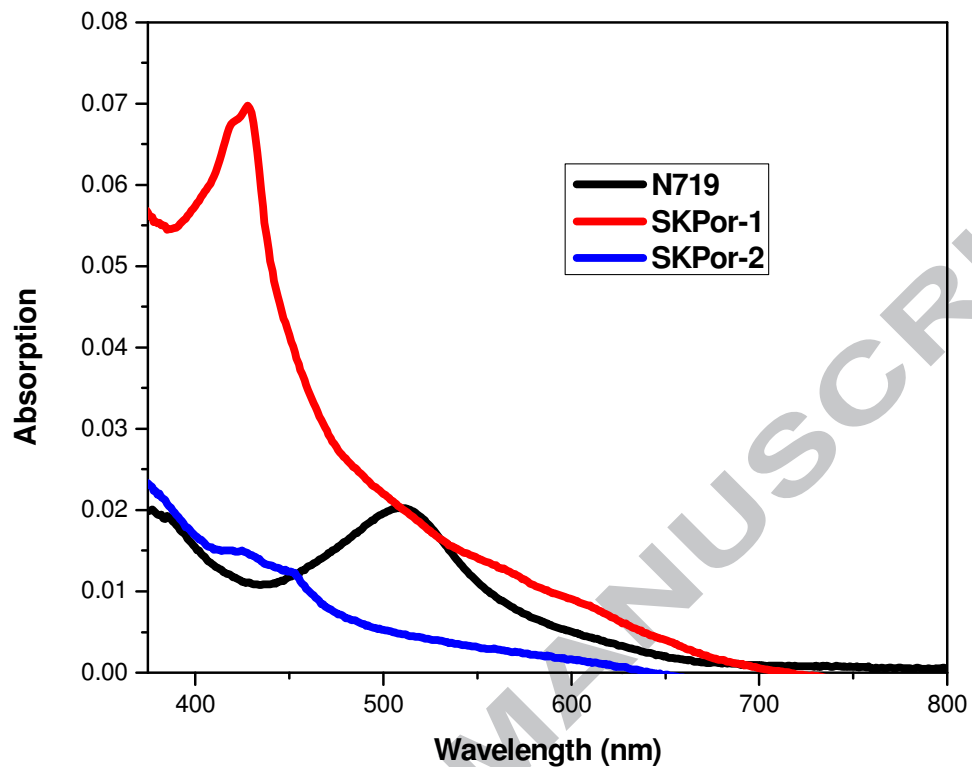


Figure.8. UV-Vis NIR absorption spectrum of dye (SKPor-1, SKPor-2 and N719 dyes) desorbed solutions.

Tables

Table-1. Absorption data of **SKPor-1** and **SKPor-2** dyes.

Table-2. The electrochemical data of **SKPor-1** and **SKPor-2** dyes.

Table 3: Comparison of Zn-Porphyrin (dimethylaminophenyl and thienyl based donor group) sensitizers and their efficiencies.

Table-4. J-V characteristics of the **SKPor-1** and **SKPor-2** sensitizers and **N719** Sensitized solar cell with liquid electrolyte under AM 1.5 irradiation condition.

Table-5. The amount of dyes adsorbed on TiO_2 surface.

ACCEPTED MANUSCRIPT

Table-1. Absorption data of SKPor-1 and SKPor-2 dyes.

Dyes	Absorption Maximum (nm)	Molar Extinction Coefficient ($\epsilon/10^5 \text{ M}^{-1}\text{Cm}^{-1}$)
SKPor-1	308, 483, 650	2.08, 0.42 , 0.45
SKPor-2	374, 376, 619	1.68 ,0.29, 0.21

Table-2. The electrochemical data of **SKPor-1** and **SKPor-2** dyes.

Dyes	Oxidation (V)	Reduction (V)	HOMO (eV)	LUMO (eV)
SKPor-1	-0.72, 0.17, 1.14	-0.85, 0.11, 1	-5.79	-3.03
SKPor-2	1.24, 1.49	-0.32, -0.88	-6.09	-3.20

Table 3: Comparison of Zn-Porphyrin (dimethylaminophenyl and thienyl based donor group) sensitizers and their efficiencies.

Serial No	Dye Name	Efficiency (%)	Reference
1	Trans - 2S2A Liyang Luo, et al.	1.8	[37]
2	Trans - 2S2A Ram Ambre, et al	0.8	[38]
3	SKPor-2	2.5	Present work
4	SKPor-1	3.2	Present work

Table-4. J-V characteristics of the **SKPor-1** and **SKPor-2** sensitizers and **N719** Sensitized solar cell with liquid electrolyte under AM 1.5 irradiation condition.

S. No	Dyes	J_{sc} (mA/cm²)	V_{oc} (V)	FF	Efficiency (η)
1	SKPor-1	9.62	0.68	0.50	3.2 %
2	SKPor-2	7.2	0.68	0.51	2.5 %
3	N719	9.0	0.67	0.57	3.4 %

ACCEPTED MANUSCRIPT

Table-5. The amount of dyes adsorbed on TiO₂ surface.

Dyes	Initial Absorption of dye solutions (0.5mM)	Molar Extinction Coefficient ($\epsilon/10^5 \text{ M}^{-1}\text{Cm}^{-1}$)	Absorption of desorbed dye solutions	Amount of Dyes adsorbed on TiO₂ surface
SKPor-1	3.70	0.74	0.06	$8.1 \times 10^{-8} \text{M Cm}^{-2}$
SKPor-2	2.14	0.42	0.01	$2.3 \times 10^{-8} \text{M Cm}^{-2}$
N719	3.47	0.69	0.02	$2.8 \times 10^{-8} \text{M Cm}^{-2}$



ACCEPTED MANUSCRIPT

Highlights

- Two different donor modified Zn-Porphyrin dyes have been designed and synthesized.
- Absorption and Cyclic voltammetry analysis reveals the dye molecules contain excellent molar extinction coefficients and HOMO-LUMO values.
- Solar cell performance of the synthesized dye almost equal to the commercial dye.

ACCEPTED MANUSCRIPT